



Analysis of the solar coronal green line profiles from eclipse observations

Maya Prabhakar^{1*}, K.P. Raju^{1†} and T. Chandrasekhar^{2‡}

¹ *Indian Institute of Astrophysics, Bangalore, India*

² *Physical Research Laboratory, Ahmedabad, India*

15th October 2018

Abstract. Analysis of the solar coronal green line profiles reveals information regarding the physical conditions of the solar corona like temperature, density, Doppler velocity, non-thermal velocity etc. It provides insights to the unresolved problems like the coronal heating and the acceleration of the solar winds. Recent studies have reported excess blueshifts in the coronal line profiles and are interpreted as due to nanoflare heating, type II spicules and nascent solar wind flow. We have analyzed a time series of Fabry-Perot interferograms of the solar corona obtained during the total solar eclipse of 2001 June 21 from Lusaka, Zambia. The spatial behavior of the coronal green line profiles were examined and variations in intensity, linewidth, Doppler velocity and line asymmetry were obtained. Several line profiles showed asymmetry indicating the presence of multicomponents. Such line profiles were fitted with double Gaussian curves. It has been found that 42% of the line profiles were single components, 34% were blueshifted, and 24% were red shifted. The secondary component of a typical line profile with blue asymmetry is found to have a relative intensity about 0.26, Doppler velocity around -30 km/s and a halfwidth about 0.65Å.

Keywords : Sun: corona - Sun: EUV radiation - line: profiles - methods

1. Introduction

The solar corona has very high temperatures of the order of millions of degrees. The basic problem posed by the discovery of the coronal temperature is to find the mechanism responsible

*email: mayap575@gmail.com

†email: kpr@iiap.res.in

‡email: chandra@prl.res.in

for heating these layers by non-thermal energy transport which has remained an enigma since its discovery in 1940. Various mechanisms like magnetoacoustic waves, Alfvén waves, magnetic reconnection, nanoflares, type-II spicules etc, constrained by velocity spectrum related to the magnetic field are attributed to cause the coronal heating.

Study of the emission coronal spectrum provides useful information regarding the physical conditions of the solar corona like temperature, density, Doppler velocity and non-thermal velocity. This may also provide insights to the unresolved mysteries like coronal heating and acceleration of solar winds. The emission coronal green line FeXIV 5302.86 Å is the strongest and widely studied line as its formation temperature (2 MK) is close to the average temperature of the inner solar corona. The presence of mass motions can change the shape of the line profiles. Raju (1998) reports the interconnection between the presence of loops in the solar corona and the structure of their line profiles.

Analysis of the coronal spectral lines was limited in the pre-Solar and Heliospheric Observatory (SOHO) era due to instrumental limitations (Domingo et al. 1995). The Coronal Diagnostic Spectrometer (CDS) lacked a good spectral resolution (Harrison et al. 1995) and Solar Ultraviolet Measurement of Emitted Radiation (SUMER) did not possess appreciable signal-to-noise ratio. Later the Extreme ultraviolet Imaging Spectrometer (EIS, Korendyke et al. 2006; Culhane et al. 2007) on board Hinode solar space observatory (Kosugi et al. 2007), in spite of having a low spectral resolution of 4000, enabled detailed study of the coronal line profiles due to good signal-to-noise ratio.

Many earlier coronal observations have reported small or no velocities and mass motions (Liebenberg, Bessey & Watson 1975; Singh, Bappu & Saxena 1982), while several others have reported large velocities and mass motions (Delone & Makarova 1969; Desai, Chandrasekhar & Angreji 1982; Raju et al. 1993). The SOHO and Transition Region and Coronal Explorer (TRACE) resolved this controversy by demonstrating that the solar atmosphere is much more variable and dynamic (Brekke 1999). Multiple flows were observed in active region by Kjeldseth-Moe et al. (1988, 1993). De Pontieu (2009) finds that the non-thermal energy is insufficient to heat the coronal plasma to millions of degrees. Observations from Hinode and SOHO reveal significant coronal mass supply from the chromosphere showing ubiquitous upflows of velocities of the order of 50-100 km/s. These upflows are chromospheric jets named as type-II spicules. Data from EIS onboard Hinode reports strong blueshifts upto 50 km/s at the footpoints of the loops in the active regions (Peter 2010). Brekke (1999) on the other hand, reports that the emission lines in the solar transition region are redshifted on an average.

Analysis of coronal green line profiles by Raju et al. (2011) shows excess blueshifts. Our study, a continuation of the latter involves the analysis of a series of Fabry-Perot interferograms of the total solar eclipse of June 21, 2001 obtained from Lusaka, Zambia. The magnitude of this eclipse was 1.0495. The data, analysis steps, results and conclusions are described in the following sections.

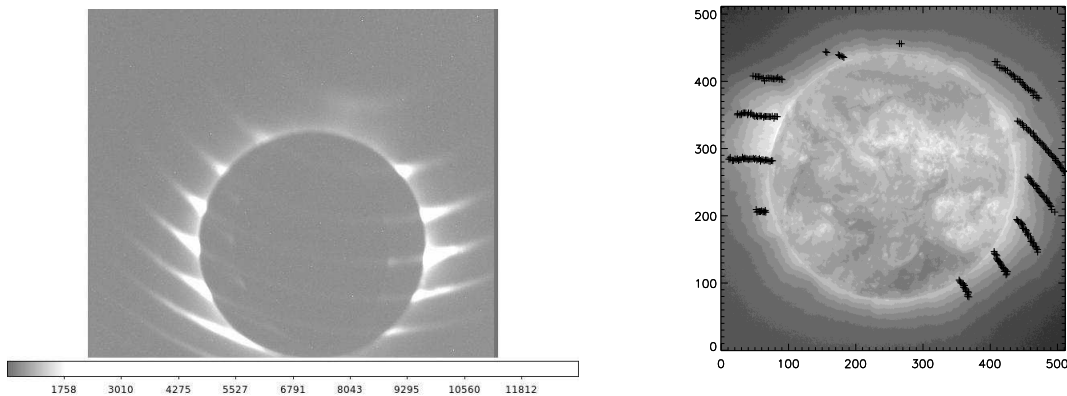


Figure 1. Left: A typical Fabry-Perot interferogram, right: Spatial locations of the line profiles plotted on the EIT image of the Sun

2. Data and analysis

The instrumentation is similar to that used by Chandrasekhar et al. (1984). The free spectral range is 4.95 \AA and the instrumental width is 0.2 \AA . The spectral resolution of the coronal green line is 26,000. The pixel size of the interferogram is 8 arc-sec. One of the interferogram we have analyzed is shown in Figure 1 (left). The analysis involves the following steps: (1) Locating the fringe center and the solar center in the interferogram, (2) Radial scans from the fringe center, (3) Positional identification of the corona, (4) Wavelength calibration, (5) Continuum subtraction, and (6) Gaussian fitting to the line profiles. We obtained around 170 line profiles in the spectral range of $1.0\text{-}1.46 R_{\odot}$ in a position angle coverage of 240° by radially scanning the interferograms. The line profiles were initially fitted with single Gaussian. The asymmetry in the line profiles is studied by determining the centroid, the mean position of the wavelength that divides the area of the line profile into two. Line profiles with multicomponents were fitted with double Gaussian curves to study their shifts.

3. Results and discussions

The spatial locations of the analyzed line profiles are plotted on the Extreme ultraviolet Imaging Telescope (EIT) image of the Sun in Figure 1 (right), where north is up and west is to the right. Among the observed line profiles, 42% were single components with negligible shifts, 34% were blueshifted and 24% were redshifted. The asymmetric line profiles being greater in number than the symmetric ones, in general indicate the presence of multicomponents in coronal green line profiles. The presence of blueshifts was first pointed out by Raju et al. (1993). Later the multicomponents were explained in terms of mass motions in the coronal loops (Raju 1999). Our results agrees well with these observations. Histograms of width, Doppler velocity and centroid are shown in Figure 2. It can clearly be seen that the histograms of Doppler velocity and centroid

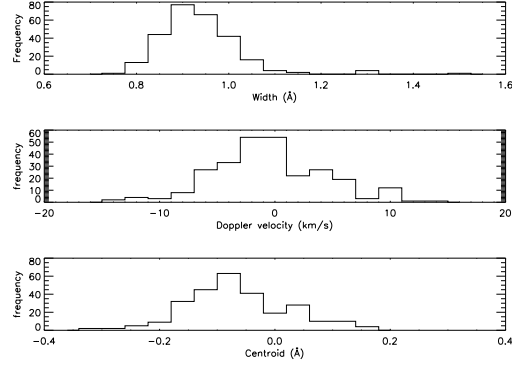


Figure 2. Histograms of width, Doppler velocity and centroid

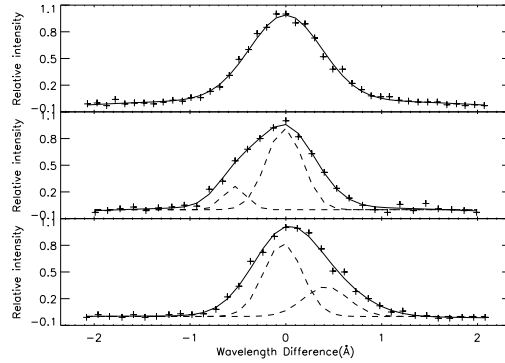


Figure 3. Gaussian fitting to the line profiles. Details are given in Table 1.

show excess blueshifts. The width peaks at 0.9 \AA , which when converted to temperature is 3.14 MK . As the formation temperature of the line is 2 MK , this implies a non-thermal velocity of 20 km/s . The Gaussian fittings of the line profiles is shown in Figure 3. Those with single components were fitted with single Gaussian curves as shown in the first panel. Profiles showing asymmetry and larger Doppler velocity were fitted with double Gaussian curves. The second panel shows a profile with excess blueshift. The secondary component in it is found to have a relative intensity around 0.26 , Doppler velocity around -30 km/s and a width around 0.65 \AA . Similarly, the third panel shows a profile with excess redshift. The red-shifted secondary component has a relative intensity around 0.33 , Doppler velocity around -23 km/s and a width of 1.27 \AA . Details of the Gaussian fitting can be seen in Table 1. The differential rotation of the Sun causes preferential blueshifts to the east limb and redshifts to the west limb. But, the velocity which is just around 2 km/s is comparable to the error involved (Raju et al. 2011). However, recent observations from SOHO and Hinode shows predominant blueshifts in the EUV region (Hara et al. 2008; De Pontieu et al. 2009; Peter 2010) which have been explained due to type-II spicules

No.	Single Gaussian			Blue			Red		
	Int	Vel	Wid	Int	Vel	Wid	Int	Vel	Wid
1	0.95	-0.08	1.24						
2	0.92	-0.90	1.03	0.26	-30.15	0.65			
3.	0.83	-1.69	1.10				0.33	23.59	1.27

Table 1. Details of Gaussian fitting. Row 1 gives the parameters of single Gaussian fitting. Row 2 gives the parameters of double Gaussian fitting with a blue component. Row 3 gives the parameters of double Gaussian fitting with a red component.

and nascent solar wind flow (Tu et al. 2005; Tian et al. 2010). Possible explanations of the multicomponents are wave motions, mass motions in coronal loops, type II spicules or nascent solar wind flow.

4. Conclusions

A detailed analysis has shown that the coronal green line profiles, in general, contain multicomponents. The excess blueshifts over redshifts in the line profiles agrees with the recent Hinode findings. The observed non-thermal velocities agrees well with the earlier reported results. The secondary component of a typical line profile with blue asymmetry is found to have a relative intensity about 0.26, Doppler velocity around -30 km/s and a halfwidth about 0.65Å. The causes for the line profile asymmetry is expected to be further probed from Hinode observations.

References

- De Pontieu, B., McIntosh, S. W., Hansteen, V. H., & Schrijver, C. J. 2009, ApJ, 701, L1
Chandrasekhar, T., Ashok, N. M., Desai, J. N., Pasachoff, J. M., & Sivaraman, K. R. 1984, Appl Opt., 23, 508
Culhane, J. L., Harra, L. K., James, A. M., et al. 2007, Sol Phys, 243, 19
Delone, A. B., & Makarova, E. A. 1969, Sol Phys, 9, 116
Desai, J. N., Chandrasekhar, T., & Angreji, P. D. 1982, J Astrophys Astron, 3, 69
Domingo, V., Fleck, B., & Poland, A. I. 1995, Sol Phys, 162, 1
Kjeldseth-Moe, O., Brynildsen, N., Brekke, P., et al. 1988, ApJ, 334, 1066
Korendyke, C. M., Brown, C. M., Thomas, R. J., et al. 2006, Appl Opt., 45, 8674
Kosugi, T., Matsuzaki, K., Sakao, T., et al. 2007, Sol Phys, 243, 3
Liebenberg, D. H., Bessey, R. J., & Watson, B. 1975, Sol Phys, 44, 345
Raju, K. P., Desai, J. N., Chandrasekhar, T., & Ashok, N. M. 1993, MNRAS, 263, 789
Raju, K. P. 1999, Sol Phys, 185, 311
Raju, K. P., Chandrasekhar, T., & Ashok, N. M. 2011, ApJ, 736, 164
Brekke, P. 1999, Sol Phys, 190, 379
Peter, H. 2001, A&A, 374, 1108
Peter, H. 2010, A&A, 521, A51

- Singh, J., Saxena, A. K., & Bappu, M. K. V. 1982, *J Astrophys Astron*, 3, 249
Tian, H., Tu, C., Marsch, E., He, J., & Kamio, S. 2010, *ApJ*, 709, L88
Tu, C.-Y., Zhou, C., Marsch, E., et al. 2005, *Science*, 308, 519